

VU Research Portal

Relation between the contrast in time integrated dynamic speckle patterns and the power spectral density of their temporal intensity fluctuations

Draijer, M.J.; Hondebrink, E.; Larsson, M.; van Leeuwen, T.G.

published in

Optics Express
2010

DOI (link to publisher)

[10.1364/OE.18.021883](https://doi.org/10.1364/OE.18.021883)

document version

Publisher's PDF, also known as Version of record

[Link to publication in VU Research Portal](#)

citation for published version (APA)

Draijer, M. J., Hondebrink, E., Larsson, M., & van Leeuwen, T. G. (2010). Relation between the contrast in time integrated dynamic speckle patterns and the power spectral density of their temporal intensity fluctuations. *Optics Express*, 18(21), 21883-21891. <https://doi.org/10.1364/OE.18.021883>

General rights

Copyright and moral rights for the publications made accessible in the public portal are retained by the authors and/or other copyright owners and it is a condition of accessing publications that users recognise and abide by the legal requirements associated with these rights.

- Users may download and print one copy of any publication from the public portal for the purpose of private study or research.
- You may not further distribute the material or use it for any profit-making activity or commercial gain
- You may freely distribute the URL identifying the publication in the public portal ?

Take down policy

If you believe that this document breaches copyright please contact us providing details, and we will remove access to the work immediately and investigate your claim.

E-mail address:

vuresearchportal.ub@vu.nl

Relation between the contrast in time integrated dynamic speckle patterns and the power spectral density of their temporal intensity fluctuations

Matthijs J. Draijer,^{1,*} Erwin Hondebrink,¹ Marcus Larsson,²
Ton G. van Leeuwen,^{1,3} and Wiendelt Steenbergen¹

¹ Biomedical Photonic Imaging, MIRA Institute, University of Twente, the Netherlands

² University of Linköping, Department of Biomedical Engineering, Sweden

³ Biomedical Engineering & Physics, Academic Medical Center, University of Amsterdam, the Netherlands

*m.j.draijer@alumnus.utwente.nl

Abstract: Scattering fluid flux can be quantified with coherent light, either from the contrast of speckle patterns, or from the moments of the power spectrum of intensity fluctuations. We present a theory connecting these approaches for the general case of mixed static-dynamic patterns of boiling speckles without prior assumptions regarding the particle dynamics. An expression is derived and tested relating the speckle contrast to the intensity power spectrum. Our theory demonstrates that in speckle contrast the concentration of moving particles dominates over the contribution of speed to the particle flux. Our theory provides a basis for comparison of both approaches when used for studying tissue perfusion.

© 2010 Optical Society of America

OCIS codes: (170.3340) Laser Doppler velocimetry; (170.3880) Medical and biological imaging; (170.4580) Optical diagnostics for medicine; (170.1650) Coherence imaging

References and links

1. P. Vennemann, R. Lindken, and J. Westerweel, "In vivo whole-field blood velocity measurement techniques," *Exp. Fluids* **42**(4), 495–511 (2007).
2. M. J. Draijer, E. Hondebrink, T. G. van Leeuwen, and W. Steenbergen, "Review of laser speckle contrast techniques for visualizing tissue perfusion," *Lasers Med. Sci.* **24**(4), 639–651 (2009).
3. R. Bonner and R. Nossal, "Model for Laser Doppler Measurements of Blood Flow in Tissue," *Appl. Opt.* **20**(12), 2097–2107 (1981).
4. J. D. Briers and S. Webster, "Laser speckle contrast analysis LASCA): a non-scanning, full-field technique for monitoring capillary blood flow," *J. Biomed. Opt.* **1**, 174–179 (1996).
5. H. Cheng, Q. Luo, S. Zeng, S. Chen, J. Cen, and H. Gong, "Modified laser speckle imaging method with improved spatial resolution," *J. Biomed. Opt.* **8**(3), 559–564 (2003).
6. D. A. Boas and A. K. Dunn, "Laser speckle contrast imaging in biomedical optics," *J. Biomed. Opt.* **15**(1), 011109 (2010).
7. J. D. Briers and S. Webster, "Quasi real-time digital version of single-exposure speckle photography for full-field monitoring of velocity or flow fields," *Opt. Commun.* **116**, 36–42 (1995).
8. J. C. Ramirez-San-Juan, R. Ramos-Garcia, I. Guizar-Iturbide, G. Martinez-Niconoff, and B. Choi, "Impact of velocity distribution assumption on simplified laser speckle imaging equation," *Opt. Express* **16**(5), 3197–3203 (2008).
9. A. B. Parthasarathy, W. J. Tom, A. Gopal, X. Zhang, and A. K. Dunn, "Robust flow measurement with multi-exposure speckle imaging," *Opt. Express* **16**(3), 1975–1989 (2008).

10. P. Zakharov, A. Völker, A. Buck, B. Weber, and F. Scheffold, "Quantitative modeling of laser speckle imaging," *Opt. Lett.* **31**(23), 3465–3467 (2006).
11. G. E. Nilsson, T. Tenland, and P. A. Öberg, "A New Instrument for Continuous Measurement of Tissue Blood Flow By Light Beating Spectroscopy," *IEEE Trans. Biomed. Engin.* **27**(1), 12–18 (1980).
12. D. D. Duncan and S. J. Kirkpatrick, "Can laser speckle flowmetry be made a quantitative tool?" *J. Opt. Soc. Am. A* **25**(8), 2088–2094 (2008).
13. P. A. Lynn, *Electronic signals and systems* (Macmillan, London, 1986).
14. J. W. Goodman and G. Parry, *Laser Speckle and Related Phenomena* (Springer-Verlag, New York, 1975).
15. A. Serov, W. Steenbergen, and F. F. M. de Mul, "Prediction of the photodetector signal generated by Doppler-induced speckle fluctuations: theory and some validations," *J. Opt. Soc. Am. A* **18**(3), 622–630 (2001).
16. D. D. Duncan, S. J. Kirkpatrick, and R. K. Wang, "Statistics of local speckle contrast," *J. Opt. Soc. Am. A Opt. Image Sci. Vis.* **25**(1), 9–15 (2008).

1. Introduction

The speckle phenomenon is widely used for determining tissue perfusion maps [1, 2]. In general, the tissue is illuminated with coherent laser light. A fraction of the laser light interacts with moving red blood cells and obtains a Doppler shift. Doppler shifted and unshifted light which are diffusely scattered from the medium create a dynamic speckle pattern on a plane of observation. Various methods of analyzing this speckle pattern have led to two separate modalities of flux imaging. In the first modality [3] the power spectrum $P(v)$ of intensity fluctuations generated in the dynamic speckle pattern is analyzed in terms of its moments given by :

$$M_i \equiv \int_{-\infty}^{\infty} v^i P(v) dv \quad (1)$$

where the zeroth order moment ($i = 0$) is a measure for the concentration of red blood cells and the first order moment ($i = 1$) is a measure for the flux or perfusion [3]. The physics behind this modality is well-known and it has been shown by Bonner and Nossal [3] that, for low blood concentrations, the concentration of red blood cells and their average velocity are both linearly represented by the power spectral moments of equation 1.

In the second modality, referred to as laser speckle contrast methods, comprising Laser Speckle Contrast Analysis (LASCA) [4] and Laser Speckle Imaging (LSI) [5] the contrast in the speckle pattern is used as a measure for perfusion [2]. In these techniques the changing speckle pattern is averaged over a time interval in the order of the speckle decorrelation-time (i.e. in the millisecond range) leading to speckle blurring. The level of blurring is related to the movement within the illuminated medium and is quantified by the speckle contrast C , which is usually defined as the ratio of the standard deviation σ of the intensity I of the blurred image to the mean intensity $\langle I \rangle$ of the speckle pattern :

$$C \equiv \frac{\sigma}{\langle I \rangle} = \frac{\sqrt{\langle I^2 \rangle - \langle I \rangle^2}}{\langle I \rangle} \quad (2)$$

where the brackets denote spatial averaging. However, for ergodic speckle patterns, spatial and temporal averaging will give identical results.

This is the case for completely dynamic speckle patterns, hence without static component. Retrieving flux from contrast of time averaged speckle patterns lacks a generally accepted theoretical framework.

As pointed out by Boas and Dunn in their recent review [6], as yet speckle contrast flowmetry modeling has focused on retrieving velocity information of scattering particles rather than their flux which includes concentration [7–9]. The presence of a static speckle component is usually

not taken into account, with two recent exceptions [9, 10]. Already Bonner and Nossal [3] take into account the presence of a static tissue matrix, and the experimental evidence given e.g. by Nilsson et al. [11] show that laser Doppler can give a relative measurement of red cell flux within a static environment, at least for a certain range of concentrations.

Furthermore, although less problematic as long as only relative velocities are measured, models for speckle contrast flowmetry are inspired by Dynamic Light Scattering theories, implying assumptions regarding the dynamics of the particles and the associated optical intensity correlations, which is known to lead to model-dependent velocity estimations [8, 12]. Finally they often assume single scattering by moving particles.

Here we present a theory which connects the contrast in time integrated dynamic speckle patterns and the power spectral density of temporal intensity fluctuations of non-integrated speckle patterns without prior assumptions regarding the speed distribution of particles and the extent of multiple scattering. The theory includes speckle patterns with an arbitrary large static component caused by the presence of non-Doppler shifted light. We show that a contrast based parameter which is closest to the weighed spectral moments as proposed by Bonner and Nossal is $1 - C^2$. In this definition, the flux parameter will increase with increasing flow or concentration. Verification of the theory will be done by simulated speckle patterns. Linking speckle contrast flowmetry to a model based on the power spectrum of intensity fluctuations may enable quantification in terms of flux rather than velocity only.

2. Theory

We introduce time dependent function $f(t)$ which is the intensity fluctuation of a pixel, and its moving average $u(t) = \frac{1}{T} \int_{t-T}^t f(\tau) d\tau$ with T the integration time. $F(\omega)$ and $U(\omega)$ are the Fourier transforms of $f(t)$ and $u(t)$ respectively. From general Fourier transform properties for time domain shifts and integrations [13], U and F are related as

$$U(T, \omega) = \frac{1}{i\omega T} [1 - \exp(-i\omega T)] F(\omega)$$

So the relation between $F(\omega)$ and $U(\omega)$ is given by the amplitude transfer function

$$H(T, \omega) = \frac{1}{i\omega T} [1 - \exp(-i\omega T)]$$

with gain

$$|H(T, \nu)| = \frac{1}{T} \sqrt{\frac{1 - \cos(2\pi\nu T)}{2\pi^2\nu^2}}$$

and ν given in Hz. Figure 1 shows an example of $|H(T, \nu)|$ as a function of ν for integration times T of 1, 5 and 10 ms. Assume a blurred speckle pattern $I(x, t)$ in which blurring is realized by averaging a dynamic speckle pattern within window T . Assuming statistical homogeneity in time and space, this speckle pattern can be decomposed in an average value $\langle I \rangle$, a static, time independent spatial fluctuation $I_s(x)$ and a time- and space dependent fluctuation $I_T(x, t)$ which depends on the integration time T . These components are shown in Fig. 2 which features an example of a blurred intensity I along a line in x-direction. Hence $I(x, t) = \langle I \rangle + I_s(x) + I_T(x, t)$. I_s will be nonzero when part of the light producing the speckle pattern has a constant phase, for instance due to interaction with static objects only. For a static-dynamic speckle pattern, for $T \rightarrow \infty$ we obtain $I_T \rightarrow 0$. For a fully dynamic speckle pattern, $I_s(x) = 0$ while for $T \rightarrow \infty$ also $I_T(x, t) \rightarrow 0$ and $I(x, t) \rightarrow \langle I \rangle$. Substituting the above form of $I(x, t)$ in equation 2 gives :

$$C^2 = \frac{\langle (I_s + I_T)^2 \rangle}{\langle I \rangle^2} = \frac{(\langle I_s^2 \rangle + \langle I_T^2 \rangle)}{\langle I \rangle^2} \quad (3)$$

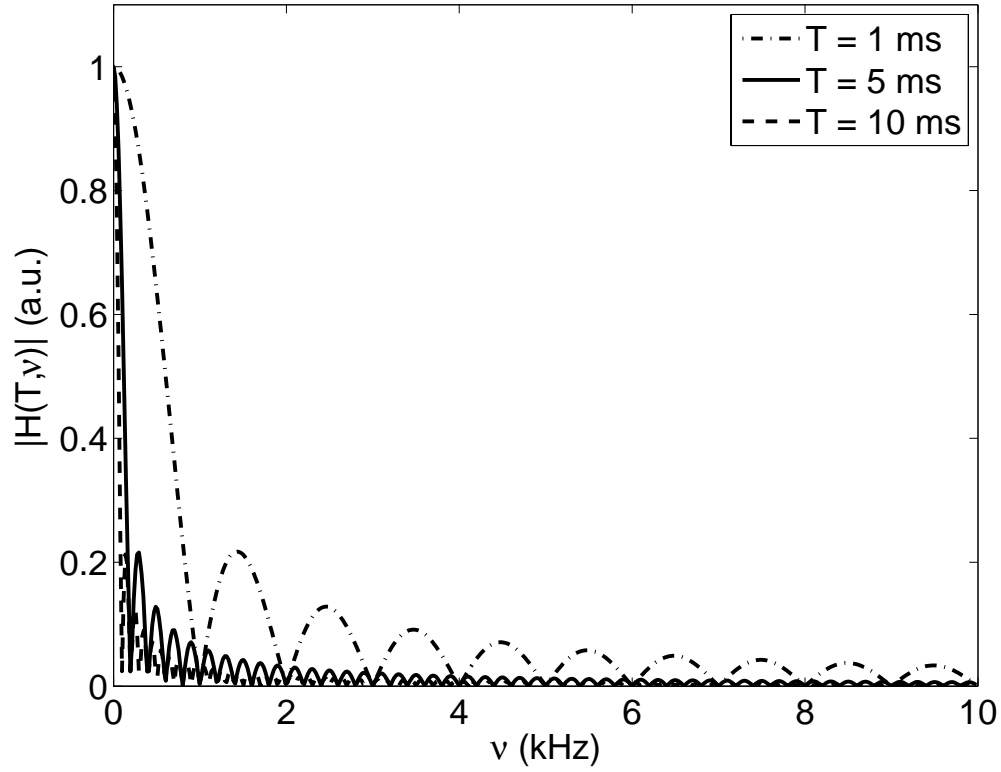


Fig. 1: Gain of transfer function $|H(T, \nu)|$ for moving average operation with integration times $T = 1, 5$ and 10 ms.

where we assumed $\langle I_s I_T \rangle = 0$, since for each possible value of I_s , positive and negative values of I_T occur.

Furthermore, contrast as a function of integration time T can be written as :

$$C^2(T) = C^2(0) + \int_0^T \frac{dC^2}{d\tilde{T}} d\tilde{T} \quad (4)$$

The intensity in an unblurred polarized speckle pattern will have an exponential probability density function [14], so $C^2(0)$ equals unity. Since in the right hand side of equation 3 only $I_T(x, t)$ depends on T , substitution of equation 3 in equation 4 gives

$$C^2(T) = 1 + \frac{1}{\langle I \rangle^2} \int_0^T \frac{\partial}{\partial \tilde{T}} \langle I_T^2 \rangle d\tilde{T} \quad (5)$$

By using Parseval's theorem and the transfer function $H(T, \nu)$, $\langle I_T^2 \rangle$ can be written as :

$$\langle I_T^2 \rangle = \int_{-\infty}^{\infty} P(\nu) |H(T, \nu)|^2 d\nu \quad (6)$$

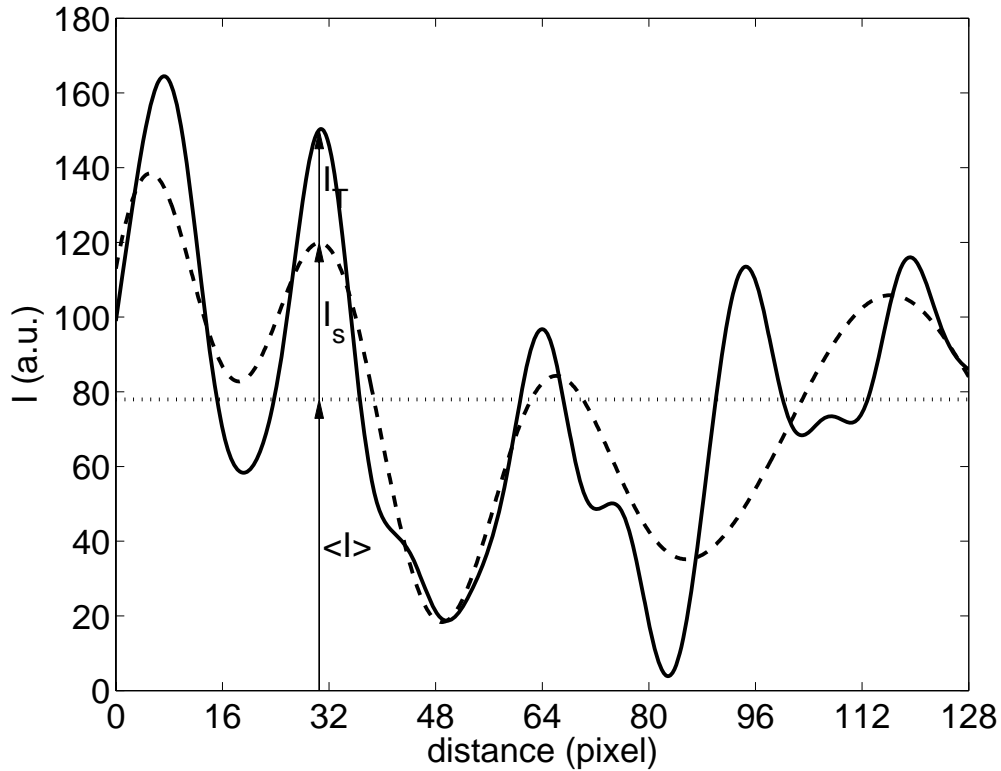


Fig. 2: Decomposition of the blurred intensity I (solid) into average value $\langle I \rangle$ (dotted), static intensity fluctuation I_s (dashed) and time-dependent blurred fluctuation I_T .

Strictly speaking Parseval's theorem implies averaging over all time in the lefthand side. Since static-dynamic speckle patterns are non-ergodic, this should be done both for regions within the speckle pattern that are bright or dark. However, averaging over all space, as indicated by $\langle \rangle$, is equivalent to temporal averaging in a limited part of space. Substituting Eq. (6) into Eq. (5) results in :

$$C^2(T) = 1 + \frac{1}{\langle I \rangle^2} \int_{-\infty}^{\infty} P(\nu) \left[|H(T, \nu)|^2 \right]_0^T d\nu \quad (7)$$

which, using Eq. (1) with $i = 0$, reduces to

$$C^2(T) = 1 - \frac{M_0}{\langle I \rangle^2} + \frac{1}{\langle I \rangle^2} \int_{-\infty}^{\infty} P(\nu) |H(T, \nu)|^2 d\nu \quad (8)$$

since $|H(0, \nu)| = 1$. Equation (8) expresses the speckle contrast in terms of the power spectrum of the local temporal intensity fluctuations in the speckle pattern. For $T \downarrow 0$, it holds that $H(T, \nu) \rightarrow 1$ for all frequencies, reducing Eq. (8) to $C^2 = 1$, which is the required value for a snapshot of the speckle pattern. For $T \rightarrow \infty$, $H(T, \nu)$ approaches zero and the last term on the right-hand side cancels out, resulting in $C^2(T \rightarrow \infty) = 1 - M_0 / \langle I \rangle^2$. For a completely dynamic speckle pattern, the property of ergodicity leads to $M_0 / \langle I \rangle^2 = 1$ so $C^2(T \rightarrow \infty) \rightarrow 0$. Hence, Eq. (8) shows the required behavior for extreme cases.

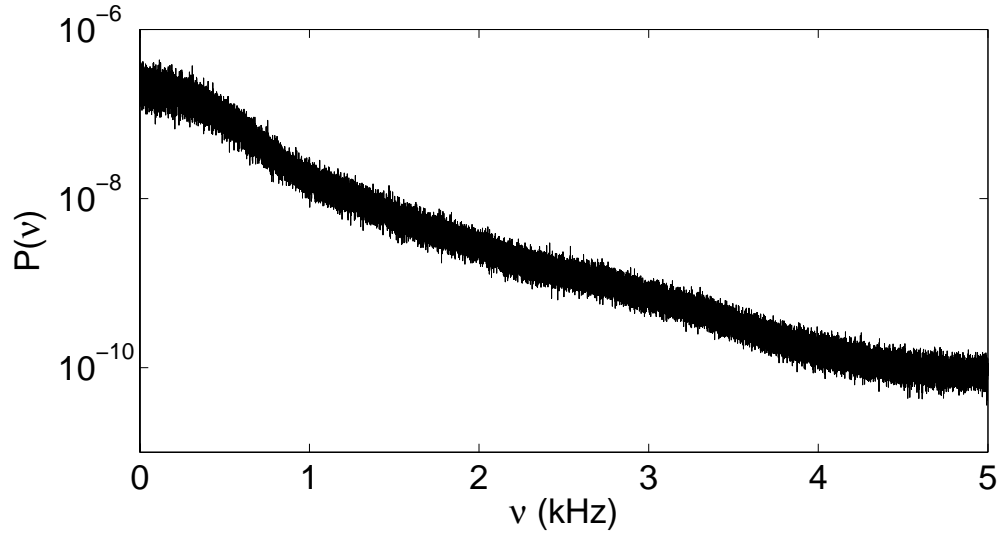


Fig. 3: Power spectrum averaged over an area of 7×7 pixels of the artificial speckle pattern used to determine the spatial contrast.

Since $M_0 / \langle I \rangle^2 = f_D(2 - f_D)$ with f_D the fraction of Doppler shifted light [15], the limiting behavior of Eq. (8) agrees with the form given by Zakharov et al. [10] for quantitative modeling of laser speckle imaging.

To validate Eq. (8), completely dynamic artificial speckle patterns are generated by making use of the concept of a copula [16]. For the speed of change of the speckle pattern, a time scale was chosen which was realistic for tissue speckle. The dynamic speckle pattern was recorded for a total duration of 12.8 seconds.

From the dynamic speckle pattern, for 10 random pixels the intensity as a function of time was extracted. Per pixel, from the time signal the temporal contrast was determined from its definition in Eq. (2). Furthermore in each pixel, from the power spectrum of the time trace the contrast was predicted for different values of T using Eq. (8).

The spatial contrast is determined in concentric regions of 7×7 pixels around 10 random pixels. In each region, the contrast was determined from the definition in Eq. (8) as well as predicted by Eq. (2) based on the averaged power spectrum in the region. An example of an averaged power spectrum over 7×7 pixels is shown in Fig. 3. The average contrast values and their standard deviations are shown in Fig. 4.

Figure 4 shows that Eq. (8) allows for prediction of both temporal and spatial speckle contrast values based on the power spectrum of the associated intensity fluctuations. There is a much better agreement between the simulated and predicted contrast-curves for the case of temporal contrast than for spatial contrast. Furthermore the error bars for temporal contrast are smaller than for spatial contrast. The discrepancy for the spatial contrast can be explained from the fact that in the limited region of interest of 7×7 pixels, the speckle pattern does not exhibit all intensity variations which are present in the complete speckle pattern. For integration times above 1 ms (i.e., which are normally used in speckle contrast techniques [2]) there is good agreement between the predicted and simulated spatial contrast values. The smaller variation of temporal contrast compared to spatial contrast can be explained from the fact that in each of the 10 randomly chosen pixels, spatial contrast is obtained from averaging over 49 pixels in the

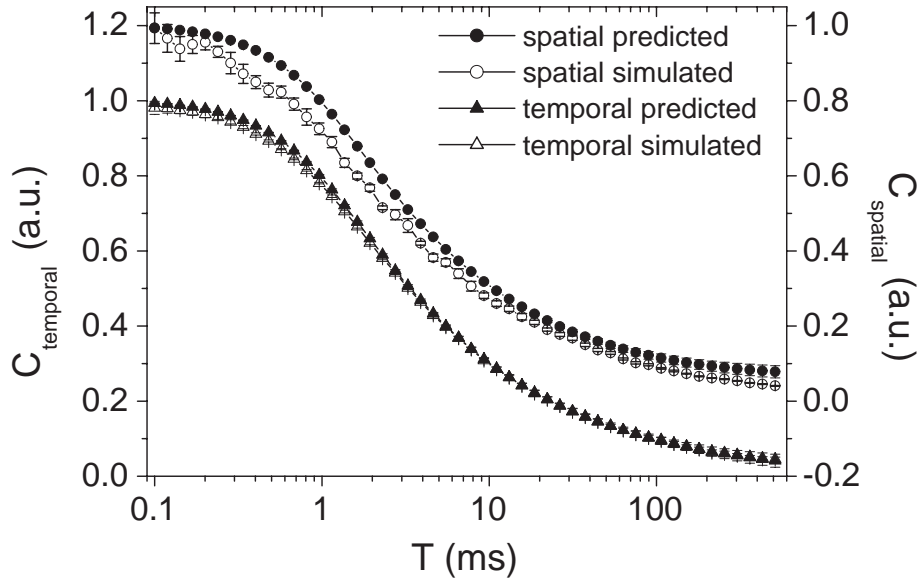


Fig. 4: Measured (open symbols) and predicted (closed symbols) speckle contrast values for temporal (squares) and spatial (circles) contrast as a function of integration time T , for artificial speckles.

surrounding region of interest, while the temporal contrast is obtained from all time points. Note the fact that for integration times > 0.5 second still the contrast did not reach zero, presumably due to low frequencies (e.g., below 1 Hz) which are present in the signal.

Given the suitability of the first order power spectral moment of intensity fluctuations as an estimator of particle flux within a static turbid matrix, as shown by Bonner and Nossal [3] for low particle flux, the expression derived in this paper for the contrast in blurred speckle forms the basis for further study of speckle contrast techniques. Here only a first step will be made. Clearly, Eq. (8) shows that speckle contrast provides an integral over the power spectrum $P(\nu)$ weighed with $|H(T, \nu)|^2$. For the contrast based flux parameter $1 - C^2$ we can derive from Eq. (8) that :

$$1 - C^2 = \frac{1}{\langle I \rangle^2} \int_{-\infty}^{\infty} \left(1 - |H(T, \nu)|^2 \right) P(\nu) d\nu \quad (9)$$

In Fig. 5 the spectral weighting function in Eq. (9) is shown for integration times of 1, 2, 5 and 15 ms, respectively. The weighting function increases nonlinearly from 0 to 1 at $\nu = 1/T$. For $\nu > 1/T$ the weighting function is almost constant, showing decaying oscillations between 1 and 0.95. Hence, for integration times $5 \text{ ms} < T < 15 \text{ ms}$ realistic for speckle contrast techniques, frequency dependent weighting is only performed in a frequency interval between 0 Hz and $67 \text{ Hz} < \nu < 200 \text{ Hz}$. For higher frequencies, $1 - C^2$ mainly provides the zero order moment of the power spectrum. For realistic integration times and for low concentrations of moving particles that are assumed in the theory of Bonner and Nossal [3], speckle contrast mainly provides information regarding the concentration of moving particles rather than their

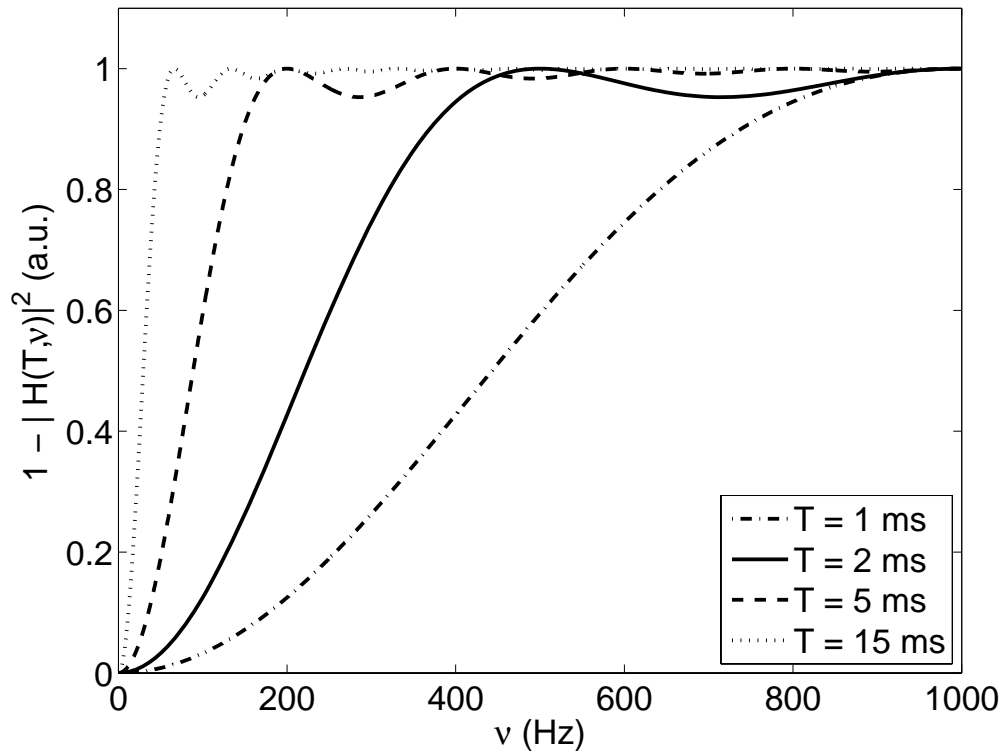


Fig. 5: Spectral weighting functions realized by $1 - C^2$, with C the contrast of integrated speckle for integration times T of 1, 2, 5 and 15 ms.

speed. Information about speed variations is only conveyed inasmuch as these variations affect the spectral broadening in the interval $0 < \nu < 1/T$ (in Hz). In this interval the frequency weighting is nonlinear, with an approximately 2nd order weighting ($\propto \nu^2$) for $\nu \rightarrow 0$. The second order weighting can be extended to higher frequencies by reducing integration time T . For instance, assuming that the spectral weighting function associated with $1 - C^2$ has a second order behavior for $0 < \nu < 1/2T$, the power spectrum shown in Fig. 3, with a width of 5 kHz which is typical for physiological perfusion, would be obtained for an integration time of approximately 0.1 ms. This will give a contrast value which is only slightly smaller than 1, and therefore will not be very sensitive. Figure 5 also suggests that speckle contrast methods will be particularly sensitive to changes in the power spectrum in the low frequency range, e.g. caused by overall tissue motion or speed variations of particles moving at a low speed. For other flux estimators which provide higher flux or velocity values for lower contrast, such as $1/C$, a similar analysis may be made, however this will be mathematically less elegant.

3. Conclusion

In this paper, we have presented a theory which expresses the contrast in time integrated dynamic speckle patterns in terms of the power spectral density of their local temporal intensity fluctuations. The theory covers mixed static-dynamic speckle patterns, provided that they are statistically homogeneous. Verification was done on computer-created fully dynamic speckle patterns.

We show that with speckle contrast C , the flux parameter $1 - C^2$ provides a weighted average of the power spectrum of photocurrent fluctuations similar to that in laser Doppler flowmetry, however with nonlinear rather than linear weighting. For very small integration times $1 - C^2$ would imply a second order weighting. For realistic integration times $T > 5$ ms, speckle contrast mainly provides information regarding the concentration of particles moving within a static matrix, with speed information only present as far as represented by the power spectrum for frequencies between zero and $1/T$ Hz. The presented theory will enable further research into the use of speckle contrast as an estimator of tissue perfusion.